Progress In Electromagnetics Research, Vol. 129, 231–250, 2012

ADAPTIVE DETECTION OF MULTIPLE POINT-LIKE TARGETS UNDER CONIC CONSTRAINTS

C. Hao[1, *], F. Bandiera[2], J. Yang[3], D. Orlando[4], S. Yan[1], and C. Hou[1]

[1]State Key Laboratory of Acoustics, Institute of Acoustics, Chinese Academy of Sciences, Beijing 100190, China

[2]Dipartimento di Ingegneria dell'Innovazione, Universita del Salento, Lecce 73100, Italy

[3]Department of Electrical and Computer Engineering, Queen's University Kingston, Canada

[4]ELETTRONICA S.p.A., Via Tiburtina Valeria, Roma 00131, Italy

Abstract—This paper addresses the problem of detecting multiple point-like targets in the presence of steering vector mismatches and Gaussian disturbance with unknown covariance matrix. To this end, we first model the actual useful signal as a vector belonging to a proper cone whose axis coincides with the whitened direction of the nominal array response. Then we develop two robust adaptive detectors resorting to the two-step GLRT-based design procedure without assignment of a distinct set of secondary data. The performance assessment has been conducted by Monte Carlo simulation, also in comparison to previously proposed detectors, and confirms the effectiveness of the newly proposed ones. In the last part of the work, in order to restore the detection performance of the newly proposed detectors in the presence of a large number of range cells contaminated by useful signals, we consider two adaptive detectors which resort to the structure information of the disturbance covariance matrix, and show that the *a-priori* information on the covariance structure can lead to a noticeable performance improvement.

Received 2 April 2012, Accepted 4 June 2012, Scheduled 21 June 2012

* Corresponding author: Chengpeng Hao (haochengp@mail.ioa.ac.cn).

1. INTRODUCTION

Adaptive radar detection of targets embedded in Gaussian disturbance has represented an active field of research in the last decades. Starting from the lack of a uniformly most powerful (UMP) test for the quoted problem, a variety of different solutions have been explored in open literature. Specifically, adaptive detection of point-like targets embedded in Gaussian disturbance has been addressed in [1–3], where it is assumed that a set of secondary data, free of signal components but sharing the spectral properties of the data under test, is available. However, these solutions may experience a performance degradation in practice wherein the actual steering vector is not consistent with the nominal one. A mismatched signal may appear subject to several causes, such as calibration and pointing errors, wavefront distortions and imperfect antenna shape. To handle such mismatched signals, an adaptive beamformer orthogonal rejection test (ABORT) is proposed, which takes into account the rejection capabilities at the design stage [4], introducing a trade off between the detection performance for mainlobe signals and rejection capabilities for sidelobe ones. Moreover, some alternative approaches are devised in [5–7], which depends on constraining the actual signature to belong to a cone, whose axis coincides with its nominal value. An important point that has emerged from the study of adaptive detection techniques under mismatched signals is the superiority of the so called "tunable detectors," i.e., algorithms capable of changing their behavior by tuning proper parameters [8–11].

All of above mentioned papers deal with the case of a single cell under test, while the detection of multiple and/or distributed targets under mismatched signal models has not received much consideration until now. It naturally arises when data are collected by high resolution radars (HRRs) [12–22] that can resolve a target into a number of scattering centers appearing into different range cells. In this context, relevant examples are [23, 24] where tunable detectors for distributed target are proposed. In addition, a customary assumption that all quoted works share is that a set of secondary data is available. Such hypothesis has been removed in [25, 26] where adaptive detection of multiple point-like targets in correlated Gaussian noise, based upon a modification of the generalized likelihood ratio test (GLRT) criterion, namely the so-called two-step GLRT-based design procedure [2], has been addressed. Therein, secondary data are selected as part of the decision process based on a priori knowledge about the maximum number of point-like targets. More precisely, in [25], the authors generalize the GLRT to the case of detecting multiple point-like targets,

whereas in [26], the ABORT idea is improved to address detection of multiple point-like targets.

This paper moves a further step: it proposes two tunable radar detectors for multiple point-like targets and without a distinct set of secondary data. More precisely, it deals with the problem of detecting an unknown signal, lying in a conic set whose axis coincides with the nominal steering vector in the whitened observation space. This model is a viable means to address adaptive detection in case of mismatched steering vectors [5–7]. The performance assessment, conducted analytically for matched and mismatched signals, highlights that the proposed detectors achieve a visible performance improvement over the existing ones, especially in the presence of severe steering vector mismatches. Nevertheless, for a large number of range cells contaminated by useful signals, the relative detection performance of the proposed detectors degrades. In order to circumvent this drawback, two persymmetric detectors based on the structure information of the disturbance covariance matrix (DCM) are proposed. More precisely, in addition to modeling the actual useful signal as a vector belonging to a proper cone, we assume that the DCM is a positive definite Hermitian and persymmetric matrix. Finally, the performance of the persymmetric detectors is analyzed and compared via Monte Carlo simulations.

The paper is organized as follows. Section 2 deals with the problem formulation and the design of the tunable detectors. The performance analysis of the aforementioned detectors is carried on in Section 3, where, in addition, two persymmetric detectors are introduced and their performances are assessed. Finally, conclusions and future research tracks are given in Section 4.

2. PROBLEM FORMULATION AND DESIGN ISSUES

Assume that data are collected from N sensors and deal with the problem of detecting the presence of a target across K range cells $\mathbf{r}_l \in \mathbb{C}^{N\times 1}$, $l \in \Omega \equiv \{1,\ldots,K\}$. Moreover, denote by $\Omega_T \subseteq \Omega$ the set indexing the range cells that might contain useful target echoes under the signal-plus-noise hypothesis (H_1); such a set is unknown at the receiver side, but for its cardinality J.

The detection problem at hand can be formulated in terms of the following binary hypotheses test

$$\begin{cases} H_0: \ \mathbf{r}_l = \mathbf{n}_l, & l \in \Omega, \\ H_1: \begin{cases} \mathbf{r}_l = \mathbf{n}_l, & l \in \Omega \backslash \Omega_T, \\ \mathbf{r}_l = \mathbf{v}_l + \mathbf{n}_l, & l \in \Omega_T \end{cases} \end{cases} \tag{1}$$

where

- the $\mathbf{n}_l$'s $\in \mathbb{C}^{N\times 1}$, $l \in \Omega$, are independent, zero-mean, complex normal vectors with covariance matrix given by $E[\mathbf{n}_l\mathbf{n}_l^\dagger] = \mathbf{M}$, $l \in \Omega$, where $E[\cdot]$ denotes expectation and † conjugate transpose;
- Ω_T is an unknown subset of Ω of cardinality J ($J \leq K$);
- $\Omega \backslash \Omega_T$ denotes the difference between Ω and Ω_T;
- $\mathbf{v}_l$, $l \in \Omega_T$, denotes the actual steering vector which might not be aligned with the nominal steering vector $\mathbf{v}_0$.

In order to facilitate the study of the problem (1), we apply a unitary transformation to bring the signal representation into a simplified form, which does not change the problem as it is equivalent to a change of coordinates. Precisely, we denote by $\mathbf{U}$ a unitary transformation such that $\mathbf{U}\mathbf{M}^{-1/2}\mathbf{v}_0$ is parallel to $\mathbf{e}_N = [0, 0, \ldots, 1]^T$ ($[\cdot]^T$ denotes the transpose operator). In the perfect matching case, it is assumed that $\mathbf{v}_{wl} = \mathbf{U}\mathbf{M}^{-1/2}\mathbf{v}_l = \alpha_l\mathbf{e}_N$, $l \in \Omega_T$, with α_l an unknown complex parameter accounting for the channel propagation effects as well as the target reflectivity.

In order to face with possible mismatched signals, we assume that $\mathbf{v}_l$ is not perfectly known. In particular, at the design stage, we suppose that $\mathbf{v}_{wl}$ belongs to the set Γ (see Fig. 1) defined as follows [5]:

Definition: Let $\mathbf{x} = (\mathbf{x}_1^T, x_N)^T$ be an N-dimensional complex vector with last component x_N, then

$$\Gamma = \left\{\mathbf{x} = \left(\mathbf{x}_1^T, x_N\right)^T \in \mathbb{C}^{N\times 1} : ||\mathbf{x}_1|| \leq \gamma |x_N|\right\},$$

where $||\cdot||$ denotes the Euclidean norm of a complex vector, and $|\cdot|$ is the modulus of a complex number. Observe that γ is a design parameter

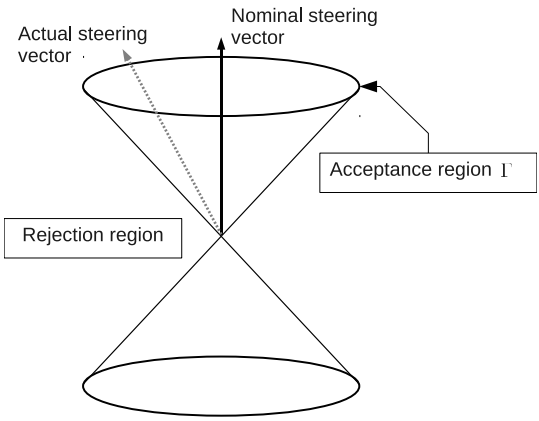

Figure 1. Pictorial description of the acceptance and rejection regions of test (1).

and that it should be set based upon the possible a priori knowledge about the mismatch.

A possible way to solve test (1) is to resort to the two-step GLRT-based design criterion [2]. In the first step, derive the GLRT over the $\mathbf{r}_l$'s, $l \in \Omega$, assuming that $\mathbf{M}$ is known. Fully adaptive detectors are then obtained by substituting the unknown matrix by a proper estimate. Following this rationale in the sequel we design two robust detectors for the problem at hand.

2.1. Conic-Acceptance GLRT

The GLRT for test (1), under the assumption that $\mathbf{M}$ is known, is given by

$$\frac{\max\limits_{\Omega_T} \max\limits_{\{\mathbf{v}_{wl}\in\Gamma\}_{l\in\Omega_T}} f(\mathbf{r}_1,\ldots,\mathbf{r}_K|\Omega_T,\{\mathbf{v}_l\}_{l\in\Omega_T},\mathbf{M},H_1)}{f(\mathbf{r}_1,\ldots,\mathbf{r}_K|\mathbf{M},H_0)} \underset{H_0}{\overset{H_1}{\gtrless}} \eta, \tag{2}$$

where

$$f(\mathbf{r}_1,\ldots,\mathbf{r}_K|\mathbf{M},H_0) = \left[\frac{1}{\pi^N \det(\mathbf{M})}\right]^K \exp\left\{ -\sum_{l\in\Omega} \mathbf{r}_l^\dagger \mathbf{M}^{-1}\mathbf{r}_l \right\} \tag{3}$$

and

$$f(\mathbf{r}_1,\ldots,\mathbf{r}_K|\Omega_T,\{\mathbf{v}_l\}_{l\in\Omega_T},\mathbf{M},H_1) = \left[\frac{1}{\pi^N \det(\mathbf{M})}\right]^K$$
$$\times\exp\left\{ -\sum_{l\in\Omega\setminus\Omega_T} \mathbf{r}_l^\dagger \mathbf{M}^{-1}\mathbf{r}_l - \sum_{l\in\Omega_T} (\mathbf{r}_l-\mathbf{v}_l)^\dagger \mathbf{M}^{-1}(\mathbf{r}_l-\mathbf{v}_l) \right\} \tag{4}$$

are the probability density functions (pdfs) of $\mathbf{r}_1,\ldots,\mathbf{r}_K$ under H_0 and H_1, respectively, with $\det(\cdot)$ the determinant of a square matrix, and η is the threshold value to be set in order to ensure the desired probability of false alarm (P_{fa}).

Substituting (3) and (4) in (2), after some algebraic manipulations, the natural logarithm of left-hand side of (2) can be recast as

$$\max_{\Omega_T} \left[-\min_{\{\mathbf{v}_{wl}\in\Gamma\}_{l\in\Omega_T}} \sum_{l\in\Omega_T} (\mathbf{r}_l-\mathbf{v}_l)^\dagger \mathbf{M}^{-1}(\mathbf{r}_l-\mathbf{v}_l) + \sum_{l\in\Omega_T} \mathbf{r}_l^\dagger \mathbf{M}^{-1}\mathbf{r}_l \right]. \tag{5}$$

The minimization over $\{\mathbf{v}_{wl}\in\Gamma\}_{l\in\Omega_T}$ can be accomplished in closed form exploiting the results in [5, 23], i.e.,

$$\min_{\{\mathbf{v}_{wl}\in\Gamma\}_{l\in\Omega_T}} \sum_{l\in\Omega_T} (\mathbf{r}_l-\mathbf{v}_l)^\dagger \mathbf{M}^{-1}(\mathbf{r}_l-\mathbf{v}_l) = \sum_{l\in\Omega_T} \frac{a_l^2 u(b_l)}{1+\gamma^2},$$

where $u(\cdot)$ is the unit step function, and

$$a_l = \sqrt{\mathbf{r}_l^\dagger \mathbf{M}^{-1}\mathbf{r}_l - \frac{|\mathbf{v}_0^\dagger \mathbf{M}^{-1}\mathbf{r}_l|^2}{\mathbf{v}_0^\dagger \mathbf{M}^{-1}\mathbf{v}_0}} - \gamma\sqrt{\frac{|\mathbf{v}_0^\dagger \mathbf{M}^{-1}\mathbf{r}_l|^2}{\mathbf{v}_0^\dagger \mathbf{M}^{-1}\mathbf{v}_0}},$$

$$b_l = \mathbf{r}_l^\dagger \mathbf{M}^{-1}\mathbf{r}_l - \frac{|\mathbf{v}_0^\dagger \mathbf{M}^{-1}\mathbf{r}_l|^2}{\mathbf{v}_0^\dagger \mathbf{M}^{-1}\mathbf{v}_0}\left(1+\gamma^2\right).$$

This implies that the GLRT can be written as

$$\max_{\Omega_T} \sum_{l\in\Omega_T} \left[\mathbf{r}_l^\dagger \mathbf{M}^{-1}\mathbf{r}_l - \frac{1}{1+\gamma^2} a_l^2 u(b_l)\right] \underset{H_0}{\overset{H_1}{\gtrless}} \eta, \tag{6}$$

where η is a suitable modification of the original threshold.

Finally, maximization over the unknown set Ω_T can be easily obtained selecting $\widehat{\Omega}_T$ as the set of integers indexing the range cells in Ω, which correspond to the greatest values of

$$\mathbf{r}_l^\dagger \mathbf{M}^{-1}\mathbf{r}_l - \frac{1}{1+\gamma^2} a_l^2 u(b_l), \quad l \in \Omega.$$

The GLRT is thus given by

$$\sum_{l\in\widehat{\Omega}_T} \left[\mathbf{r}_l^\dagger \mathbf{M}^{-1}\mathbf{r}_l - \frac{1}{1+\gamma^2} a_l^2 u(b_l)\right] \underset{H_0}{\overset{H_1}{\gtrless}} \eta. \tag{7}$$

The most natural estimator of $\mathbf{M}$ in Gaussian disturbance is the sample covariance matrix (SCM) [1, 2]

$$\mathbf{S} = \frac{1}{K}\sum_{l\in\Omega} \mathbf{r}_l \mathbf{r}_l^\dagger. \tag{8}$$

Plugging $\mathbf{S}$ in place of $\mathbf{M}$ in (7), the GLRT, referred to in the following as Robust-Conic-Acceptance-GLRT (RCA-GLRT), can be written as

$$\sum_{l\in\widehat{\Omega}_T} \left[\mathbf{r}_l^\dagger \mathbf{S}^{-1}\mathbf{r}_l - \frac{1}{1+\gamma^2} c_l^2 u(d_l)\right] \underset{H_0}{\overset{H_1}{\gtrless}} \eta, \tag{9}$$

where

$$c_l = \sqrt{\mathbf{r}_l^\dagger \mathbf{S}^{-1}\mathbf{r}_l - \frac{|\mathbf{v}_0^\dagger \mathbf{S}^{-1}\mathbf{r}_l|^2}{\mathbf{v}_0^\dagger \mathbf{S}^{-1}\mathbf{v}_0}} - \gamma\sqrt{\frac{|\mathbf{v}_0^\dagger \mathbf{S}^{-1}\mathbf{r}_l|^2}{\mathbf{v}_0^\dagger \mathbf{S}^{-1}\mathbf{v}_0}},$$

$$d_l = \mathbf{r}_l^\dagger \mathbf{S}^{-1}\mathbf{r}_l - \frac{|\mathbf{v}_0^\dagger \mathbf{S}^{-1}\mathbf{r}_l|^2}{\mathbf{v}_0^\dagger \mathbf{S}^{-1}\mathbf{v}_0}\left(1+\gamma^2\right),$$

and $\widehat{\Omega}_T$ denotes the set of integers indexing the range cells in Ω which correspond to the greatest values of

$$\mathbf{r}_l^\dagger \mathbf{S}^{-1} \mathbf{r}_l - \frac{1}{1+\gamma^2} c_l^2 u(d_l), \quad l \in \Omega.$$

In particular, for $\gamma = 0$, we obtain the two-step GLRT for multiple point-like targets [25].

2.2. Conic-Acceptance ABORT

According to the orthogonal rejection criterion [4], we assume that under H_0 the received signal contains a fictitious signal which is orthogonal to the nominal steering vector $\mathbf{v}_0$ in the whitened space (see Fig. 2). Otherwise stated, the H_0 hypothesis of test (1) can be formulated as follows

$$H_0 : \begin{cases} \mathbf{r}_l = \mathbf{n}_l, & l \in \Omega \backslash \Omega_T, \\ \mathbf{r}_l = \mathbf{x}_l + \mathbf{n}_l, & l \in \Omega_T \end{cases} \tag{10}$$

where $\mathbf{x}_l$'s $\in \mathbb{C}^{N\times 1}$, $l \in \Omega_T$, are fictitious vectors, which can be expressed as $\mathbf{x}_l = \mathbf{W}\mathbf{p}_l$ with $\mathbf{p}_l \in \mathbb{C}^{(N-1)\times 1}$, $\mathbf{W} \in \mathbb{C}^{N\times(N-1)}$ is a full-column-rank matrix such that

$$\left\langle \mathbf{M}^{-1/2}\mathbf{W} \right\rangle^\perp = \left\langle \mathbf{M}^{-1/2}\mathbf{v}_0 \right\rangle. \tag{11}$$

In (11), $\langle\cdot\rangle$ denotes the range space spanned by the columns of the matrix argument, and $\langle\cdot\rangle^\perp$ its orthogonal complement. Observe that the H_1 hypothesis of (1) remains unaltered.

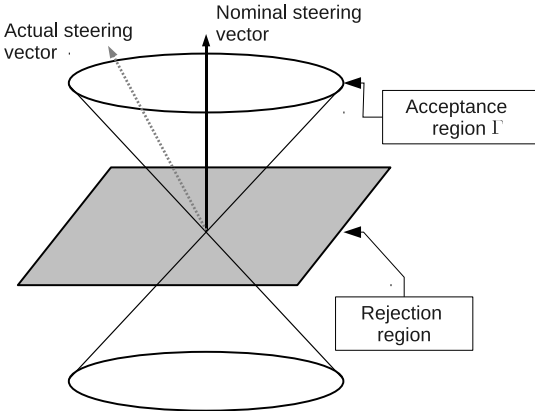

Figure 2. Pictorial description of the acceptance and rejection regions of test (1) with H_0 given by (10).

In this case, the GLRT for known $\mathbf{M}$ is given by

$$\frac{\max\limits_{\Omega_T}\max\limits_{\{\mathbf{v}_{wl}\in\Gamma\}_{l\in\Omega_T}} f(\mathbf{r}_1,\ldots,\mathbf{r}_K|\Omega_T,\{\mathbf{v}_l\}_{l\in\Omega_T},\mathbf{M},H_1)}{\max\limits_{\Omega_T}\max\limits_{\{\mathbf{p}_l\}_{l\in\Omega_T}} f(\mathbf{r}_1,\ldots,\mathbf{r}_K|\Omega_T,\{\mathbf{p}_l\}_{l\in\Omega_T},\mathbf{M},H_0)} \underset{H_0}{\overset{H_1}{\gtrless}} \eta, \tag{12}$$

where $f(\mathbf{r}_1,\ldots,\mathbf{r}_K|\Omega_T,\{\mathbf{p}_l\}_{l\in\Omega_T},\mathbf{M},H_0)$ denotes the pdf of $\mathbf{r}_1,\ldots,\mathbf{r}_K$ under the H_0 hypothesis given by (10), i.e.,

$$f(\mathbf{r}_1,\ldots,\mathbf{r}_K|\Omega_T,\{\mathbf{p}_l\}_{l\in\Omega_T},\mathbf{M},H_0)=\left[\frac{1}{\pi^N\det(\mathbf{M})}\right]^K$$
$$\times\exp\left\{-\sum_{l\in\Omega\setminus\Omega_T}\mathbf{r}_l^\dagger\mathbf{M}^{-1}\mathbf{r}_l-\sum_{l\in\Omega_T}(\mathbf{r}_l-\mathbf{W}\mathbf{p}_l)^\dagger\mathbf{M}^{-1}(\mathbf{r}_l-\mathbf{W}\mathbf{p}_l)\right\}. \tag{13}$$

Substituting (13) and (4) in (12), after some algebraic manipulations, the natural logarithm of left-hand side of (12) can be recast as

$$\min_{\Omega_T}\left[\min_{\{\mathbf{p}_l\}_{l\in\Omega_T}}\sum_{l\in\Omega_T}(\mathbf{r}_l-\mathbf{W}\mathbf{p}_l)^\dagger\mathbf{M}^{-1}(\mathbf{r}_l-\mathbf{W}\mathbf{p}_l)-\sum_{l\in\Omega_T}\mathbf{r}_l^\dagger\mathbf{M}^{-1}\mathbf{r}_l\right]$$
$$+\max_{\Omega_T}\left[\sum_{l\in\Omega_T}\mathbf{r}_l^\dagger\mathbf{M}^{-1}\mathbf{r}_l-\min_{\{\mathbf{v}_{wl}\in\Gamma\}_{l\in\Omega_T}}\sum_{l\in\Omega_T}(\mathbf{r}_l-\mathbf{v}_l)^\dagger\mathbf{M}^{-1}(\mathbf{r}_l-\mathbf{v}_l)\right] \tag{14}$$

Observe that the minimization over $\mathbf{p}_l$ can be obtained as follows [26]:

$$\min_{\{\mathbf{p}_l\}_{l\in\Omega_T}}\sum_{l\in\Omega_T}(\mathbf{r}_l-\mathbf{W}\mathbf{p}_l)^\dagger\mathbf{M}^{-1}(\mathbf{r}_l-\mathbf{W}\mathbf{p}_l)$$
$$=\sum_{l\in\Omega_T}\mathbf{r}_l^\dagger\mathbf{M}^{-1/2}(\mathbf{I}_N-\mathbf{P}_{W_w})\mathbf{M}^{-1/2}\mathbf{r}_l, \tag{15}$$

where $\mathbf{I}_N$ denotes the N-dimensional identity matrix, and $\mathbf{P}_{W_w}$ is the projector onto the subspace spanned by $\mathbf{W}_w=\mathbf{M}^{-1/2}\mathbf{W}$, i.e., $\mathbf{P}_{W_w}=\mathbf{W}_w(\mathbf{W}_w^\dagger\mathbf{W}_w)^{-1}\mathbf{W}_w^\dagger$. Moreover, condition (11) implies that

$$\mathbf{I}_N-\mathbf{P}_{W_w}=\mathbf{M}^{-1/2}\mathbf{v}_0(\mathbf{v}_0^\dagger\mathbf{M}^{-1/2}\mathbf{v}_0)^{-1}\mathbf{v}_0^\dagger\mathbf{M}^{-1/2} \tag{16}$$

and, hence, (15) becomes

$$\min_{\{\mathbf{p}_l\}_{l\in\Omega_T}}\sum_{l\in\Omega_T}(\mathbf{r}_l-\mathbf{W}\mathbf{p}_l)^\dagger\mathbf{M}^{-1}(\mathbf{r}_l-\mathbf{W}\mathbf{p}_l)=\sum_{l\in\Omega_T}\frac{|\mathbf{v}_0^\dagger\mathbf{M}^{-1}\mathbf{r}_l|^2}{\mathbf{v}_0^\dagger\mathbf{M}^{-1}\mathbf{v}_0}.$$

Thus, we conclude that the GLRT is equivalent to

$$\min_{\Omega_T}\left[\sum_{l\in\Omega_T}\left(\frac{|\mathbf{v}_0^\dagger\mathbf{M}^{-1}\mathbf{r}_l|^2}{\mathbf{v}_0^\dagger\mathbf{M}^{-1}\mathbf{v}_0}-\mathbf{r}_l^\dagger\mathbf{M}^{-1}\mathbf{r}_l\right)\right]$$
$$+\max_{\Omega_T}\left[\sum_{l\in\Omega_T}\left(\mathbf{r}_l^\dagger\mathbf{M}^{-1}\mathbf{r}_l-\frac{1}{1+\gamma^2}a_l^2u(b_l)\right)\right]\underset{H_0}{\overset{H_1}{\gtrless}}\eta. \tag{17}$$

Again, optimizations over Ω_T are straightforward and we select $\widehat{\Omega}_T^0$ and $\widehat{\Omega}_T^1$ as the sets of integers indexing the range cells in Ω, which correspond to the smallest values of

$$\frac{|\mathbf{v}_0^\dagger\mathbf{M}^{-1}\mathbf{r}_l|^2}{\mathbf{v}_0^\dagger\mathbf{M}^{-1}\mathbf{v}_0}-\mathbf{r}_l^\dagger\mathbf{M}^{-1}\mathbf{r}_l,\quad l\in\Omega$$

and the greatest values of

$$\mathbf{r}_l^\dagger\mathbf{M}^{-1}\mathbf{r}_l-\frac{1}{1+\gamma^2}a_l^2u(b_l),\quad l\in\Omega.$$

respectively. The GLRT is thus given by

$$\sum_{l\in\widehat{\Omega}_T^0}\left(\frac{|\mathbf{v}_0^\dagger\mathbf{M}^{-1}\mathbf{r}_l|^2}{\mathbf{v}_0^\dagger\mathbf{M}^{-1}\mathbf{v}_0}-\mathbf{r}_l^\dagger\mathbf{M}^{-1}\mathbf{r}_l\right)+\sum_{l\in\widehat{\Omega}_T^1}\left(\mathbf{r}_l^\dagger\mathbf{M}^{-1}\mathbf{r}_l-\frac{1}{1+\gamma^2}a_l^2u(b_l)\right)\underset{H_0}{\overset{H_1}{\gtrless}}\eta. \tag{18}$$

Finally, replacing $\mathbf{M}$ in (18) with $\mathbf{S}$, we come up with the following adaptive decision scheme, referred to in the following as Robust-Conic-Acceptance-ABORT (RCA-ABORT)

$$\sum_{l\in\widehat{\Omega}_T^0}\left(\frac{|\mathbf{v}_0^\dagger\mathbf{S}^{-1}\mathbf{r}_l|^2}{\mathbf{v}_0^\dagger\mathbf{S}^{-1}\mathbf{v}_0}-\mathbf{r}_l^\dagger\mathbf{S}^{-1}\mathbf{r}_l\right)+\sum_{l\in\widehat{\Omega}_T^1}\left(\mathbf{r}_l^\dagger\mathbf{S}^{-1}\mathbf{r}_l-\frac{1}{1+\gamma^2}c_l^2u(d_l)\right)\underset{H_0}{\overset{H_1}{\gtrless}}\eta, \tag{19}$$

where, again, $\widehat{\Omega}_T^0$ and $\widehat{\Omega}_T^1$ have to be computed using $\mathbf{S}$ in place of $\mathbf{M}$. This detector reduces to the ABORT for multiple point-like targets when $\gamma = 0$, which can be straightforwardly derived using results in [26].

3. PERFORMANCE ASSESSMENT

In this section, we carry out a performance assessment of the proposed detectors by resorting to standard Monte Carlo simulation. We assume that the mainlobe (or sidelobe) signals in different range cells have the same direction $\mathbf{v}$, and denote by ϕ the angle between the actual steering

vector and the nominal one in the whitened observation data space, i.e.,

$$\cos^2\phi = \frac{|\mathbf{v}^\dagger \mathbf{M}^{-1}\mathbf{v}_0|^2}{(\mathbf{v}^\dagger \mathbf{M}^{-1}\mathbf{v})\left(\mathbf{v}_0^\dagger \mathbf{M}^{-1}\mathbf{v}_0\right)}.$$

The term $\cos^2\phi$ is a measure of the mismatch between $\mathbf{v}$ and $\mathbf{v}_0$. Its value is one for the matched case where $\mathbf{v} = \mathbf{v_0}$, and less than one otherwise. A small value of $\cos^2\phi$ implies a large mismatch. As to the noise, it is modeled as an exponentially-correlated complex normal vector with one-lag correlation coefficient ρ, namely the (i,j)-th element of the covariance matrix $\mathbf{M}$ is given by $\rho^{|i-j|}$, with $\rho = 0.9$. In order to limit the computational burden, we assume $P_{fa} = 10^{-4}$ throughout the section. Moreover, the signal-to-noise power ratio (SNR) is defined as $\text{SNR} = \sum_{l\in\Omega_T} \mathbf{v}_l^\dagger \mathbf{M}^{-1}\mathbf{v}_l$.

The performances of the RCA-GLRT and the RCA-ABORT are analyzed in Figs. 3 and 4, respectively. In addition, we compare our detectors to their counterparts (the GLRT and the ABORT). More precisely, in the left subplot of each figure we plot P_d versus SNR for $\cos^2\phi = 1$ and several values of γ, while in the right subplot we report P_d versus $\cos^2\phi$ for the same values of γ as in Fig. 1. Moreover, both figures refer to $N = 20$, $K = 60$, $J = 5$. As it can be seen, the RCA-GLRT and the RCA-ABORT are more robust than their counterparts, although at the price of a certain loss in terms of detection of matched signals. More precisely, the higher γ, the higher the performance loss in matched signals case but, at the same time, the higher the capability

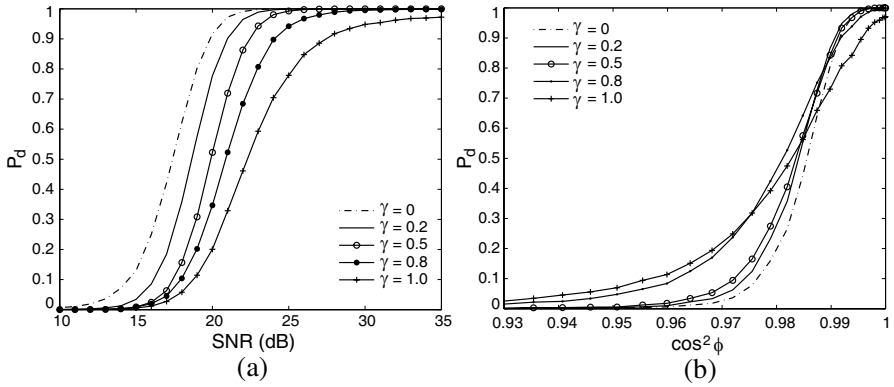

Figure 3. The performances of the RCA-GLRT with several values of γ and the GLRT ($\gamma = 0$), for $N = 20$, $K = 60$, $J = 5$, SNR = 35 dB. (a) The matched performance. (b) The mismatched performance.

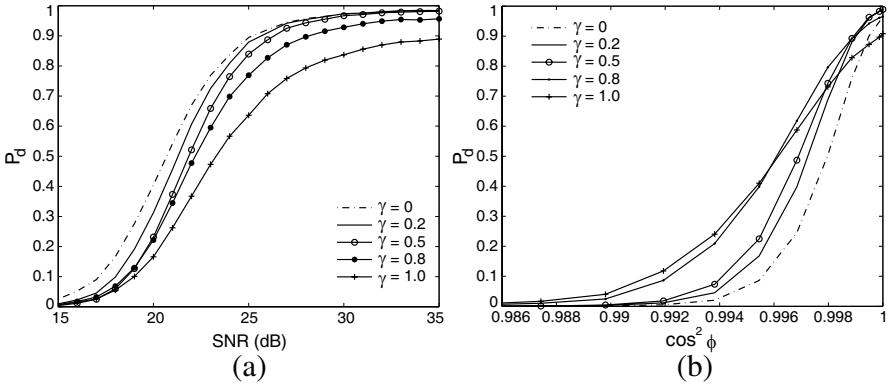

Figure 4. The performances of the RCA-ABORT with several values of γ and the ABORT ($\gamma = 0$), for $N = 20$, $K = 60$, $J = 5$, SNR $= 40$ dB. (a) The matched performance. (b) The mismatched performance.

of the receivers to detect severely mismatched signals. Otherwise stated, varying γ, we can trade target sensitivity with sidelobes energy rejection. We explicitly point out that this performance behavior agrees with the considered design criterion. Other simulation results not reported here, in order not to burden too much the analysis, have shown that the above results are still valid for other system parameters.

In Figs. 5 and 6, instead, we compare the performance of the RCA-GLRT with that of the RCA-ABORT. Fig. 5 refers to $N = 10$, $K = 40$, $J = 2$, whereas Fig. 6 assumes $N = 10$, $K = 40$, $J = 4$. Moreover, in the upper subplot of each figure, we report P_d versus SNR assuming $\cos^2 \phi = 1.0$, while, in the lower subplot, we report contours of constant P_d as functions of SNR and $\cos^2 \phi$.

Inspection of the figures highlights that for a given γ, the RCA-GLRT is more tolerant of mismatch and, therefore, less selective, whereas the RCA-ABORT is more selective and, therefore, less tolerant of mismatch. So the appropriate detector can be selected based on the system requirements. For the reader ease, in Table 1 we briefly summarize the performance shown[†] in Fig. 5. On the other hand, Figs. 5 and 6 show that a larger number of range cells contaminated by useful signals causes a performance degradation of the proposed detectors due to the fact that the estimate of $\mathbf{M}$ becomes more unreliable. Such a loss can be compensated by a knowledge-aided method which relies on the use of the structural information of the DCM. This is the subject of Section 4.

[†] Hierarchy observed in Fig. 6 is analogous to that of Fig. 5 and, hence, in order not to burden the paper, we summarize the results given in Fig. 5.

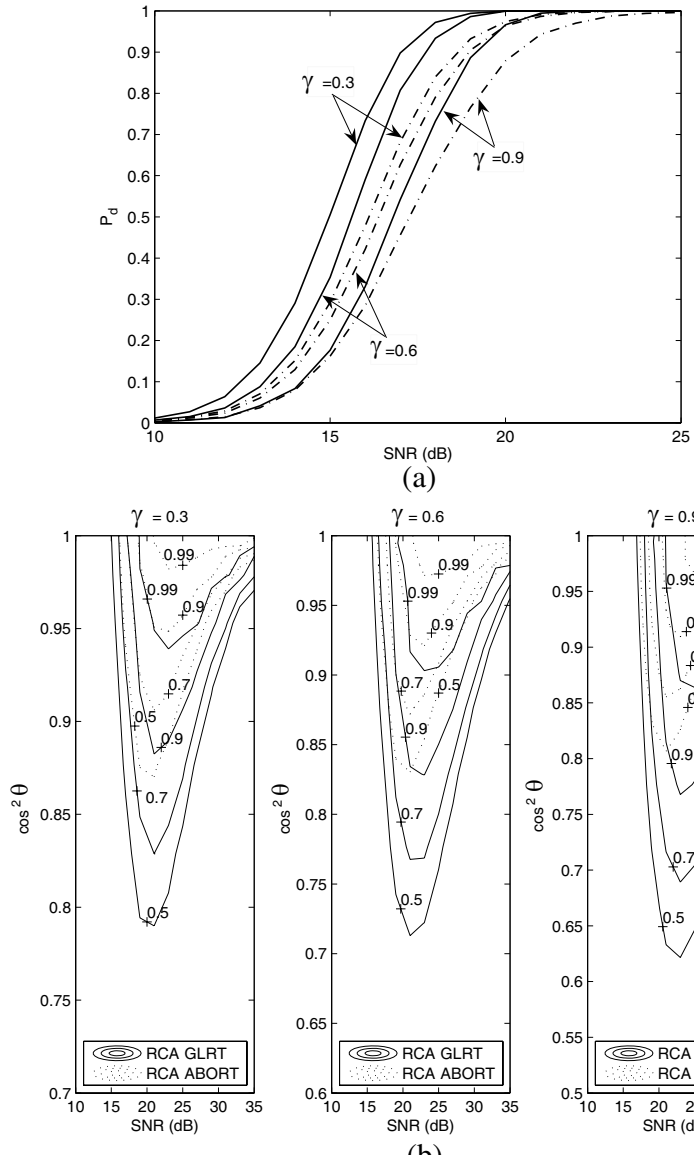

Figure 5. The performances of the RCA-GLRT (solid line) and the RCA-ABORT (dashed-dotted line), for $N = 10$, $K = 40$, $J = 2$, and several values of γ. (a) The matched performance. (b) The mismatched performance.

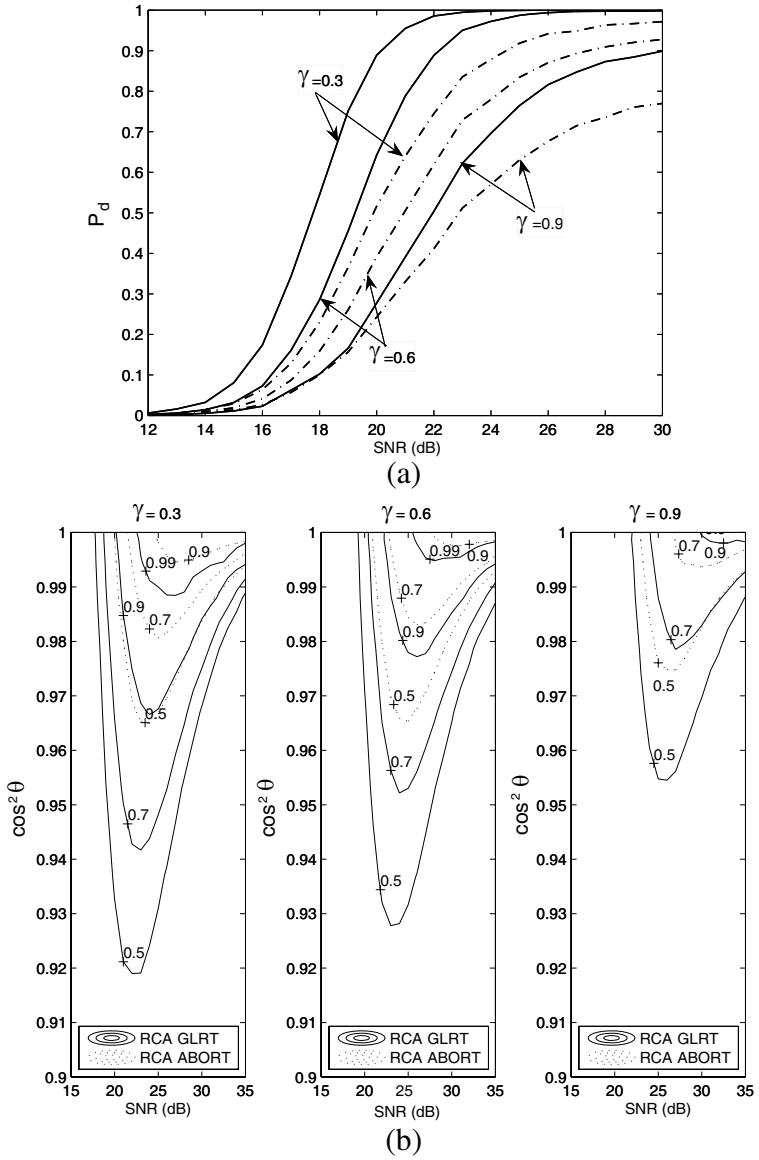

Figure 6. The performances of the RCA-GLRT (solid line) and the RCA-ABORT (dashed-dotted line), for $N = 10$, $K = 40$, $J = 4$, and several values of γ. (a) The matched performance. (b) The mismatched performance.

Table 1. Performance of the RCA-GLRT and the RCA-ABORT (SNR = 19 dB).

Matched performance			
γ	0.3	0.6	0.9
P_d of the RCA-GLRT	0.994	0.986	0.887
P_d of the RCA-ABORT	0.933	0.905	0.765
Mismatched performance			
γ	0.3	0.6	0.9
P_d of the RCA-GLRT, $\cos^2\phi = 0.9$	0.118	0.718	0.975
P_d of the RCA-ABORT, $\cos^2\phi = 0.9$	0	0.011	0.024

3.1. Persymmetric Detectors

It is clear that the estimation accuracy of $\mathbf{M}$ has an important impact on the adaptive detection performance. The SCM $\mathbf{S}$ do not take into account any prior information on the DCM structure. However many applications lead to a DCM which exhibits some particular structure, and considering this structure may lead to an improvement in both estimation and detection performance. Such a situation is frequently met in radar systems using a symmetrically spaced linear array and a symmetrically spaced pulse train for temporal domain processing [27–30]. Thus, the persymmetric structure of $\mathbf{M}$ is exploited in this section in order to improve its estimation accuracy with respect to the SCM, namely, it belongs to the set $\mathcal{P}$ defined as

$$\mathbf{M} \in \mathcal{P} \text{ if } \mathbf{M} = \mathbf{J}_N \mathbf{M}^* \mathbf{J}_N,$$

where * denotes complex conjugate, and $\mathbf{J}_N \in \mathbb{R}^{N\times N}$ is the permutation matrix, i.e.,

$$\mathbf{J}_N = \begin{bmatrix} 0 & 0 & \dots & 0 & 1 \\ 0 & 0 & \dots & 1 & 0 \\ \vdots & \vdots & \vdots & \vdots & \vdots \\ 1 & 0 & \dots & 0 & 0 \end{bmatrix}.$$

It is well known that the maximum likelihood estimation (MLE) of persymmetric covariance matrix over the $\mathbf{r}_l$'s, $l \in \Omega$, is given by [27]

$$\mathbf{S}_p = \mathbf{S} + \mathbf{J}_N \mathbf{S}^* \mathbf{J}_N / 2, \tag{20}$$

where $\mathbf{S}$ is the SCM.

Now, replacing $\mathbf{M}$ into (7) with $\mathbf{S}_p$, a fully adaptive detector, referred to in the sequel as the persymmetric RCA-GLRT (PRCA-GLRT), has the following expression

$$\sum_{l\in\widehat{\Omega}_T}\left[\mathbf{r}_l^\dagger\mathbf{S}_p^{-1}\mathbf{r}_l-\frac{1}{1+\gamma^2}e_l^2u(f_l)\right]\underset{H_0}{\overset{H_1}{\gtrless}}\eta, \tag{21}$$

where

$$e_l=\sqrt{\mathbf{r}_l^\dagger\mathbf{S}_p^{-1}\mathbf{r}_l-\frac{|\mathbf{v}_0^\dagger\mathbf{S}_p^{-1}\mathbf{r}_l|^2}{\mathbf{v}_0^\dagger\mathbf{S}_p^{-1}\mathbf{v}_0}}-\gamma\sqrt{\frac{|\mathbf{v}_0^\dagger\mathbf{S}_p^{-1}\mathbf{r}_l|^2}{\mathbf{v}_0^\dagger\mathbf{S}_p^{-1}\mathbf{v}_0}},$$

$$f_l=\mathbf{r}_l^\dagger\mathbf{S}_p^{-1}\mathbf{r}_l-\frac{|\mathbf{v}_0^\dagger\mathbf{S}_p^{-1}\mathbf{r}_l|^2}{\mathbf{v}_0^\dagger\mathbf{S}_p^{-1}\mathbf{v}_0}\left(1+\gamma^2\right)$$

and $\widehat{\Omega}_T$ denotes the set of integers indexing the range cells in Ω which correspond to the greatest values of

$$\mathbf{r}_l^\dagger\mathbf{S}_p^{-1}\mathbf{r}_l-\frac{1}{1+\gamma^2}e_l^2u(f_l),\quad l\in\Omega.$$

Similarly, plugging $\mathbf{S}_p$ in place of $\mathbf{M}$ in (18), the persymmetric RCA-ABORT (PRCA-ABORT) can be written as

$$\sum_{l\in\widehat{\Omega}_T^0}\left(\frac{|\mathbf{v}_0^\dagger\mathbf{S}_p^{-1}\mathbf{r}_l|^2}{\mathbf{v}_0^\dagger\mathbf{S}_p^{-1}\mathbf{v}_0}-\mathbf{r}_l^\dagger\mathbf{S}_p^{-1}\mathbf{r}_l\right)+\sum_{l\in\widehat{\Omega}_T^1}\left(\mathbf{r}_l^\dagger\mathbf{S}_p^{-1}\mathbf{r}_l-\frac{1}{1+\gamma^2}e_l^2u(f_l)\right)\underset{H_0}{\overset{H_1}{\gtrless}}\eta, \tag{22}$$

where, $\widehat{\Omega}_T^0$ and $\widehat{\Omega}_T^1$ correspond to the smallest values of

$$\frac{|\mathbf{v}_0^\dagger\mathbf{S}_p^{-1}\mathbf{r}_l|^2}{\mathbf{v}_0^\dagger\mathbf{S}_p^{-1}\mathbf{v}_0}-\mathbf{r}_l^\dagger\mathbf{S}_p^{-1}\mathbf{r}_l,\quad l\in\Omega$$

and the greatest values of

$$\mathbf{r}_l^\dagger\mathbf{S}_p^{-1}\mathbf{r}_l-\frac{1}{1+\gamma^2}e_l^2u(f_l),\quad l\in\Omega.$$

respectively.

In Fig. 7, we show the matched performances of the PRCA-GLRT and RCA-GLRT for $N=10$, $J=4$, $\gamma=0.6$, and several values of K, while in Fig. 8 we compare the matched performance of the PRCA-ABORT with that of the RCA-ABORT for the same system parameters as in Fig. 7. The curves highlight that for a small number of range cells, the PRCA-GLRT and PRCA-ABORT significantly outperform their unstructured counterparts. However, the gain reduces as K increases

and, for $K = 80$, the matched performances of the two receivers and their unstructured counterparts are practically coincident, due to the fact that the estimate of $\mathbf{M}$ becomes more reliable. In Table 2, we summarize the performance observed in Figs. 7 and 8.

Finally, two remarks are now in order. First, the newly proposed detectors guarantee the CFAR property with respect to $\mathbf{M}$. Proofs of such statements, not reported here for the sake of brevity, follow the lead of [23] and references therein. Second, if the DCM has not the persymmetric property, the performance of the persymmetric detectors will greatly deteriorate.

Table 2. Performance of the PRCA-GLRT and the PRCA-ABORT ($\gamma = 0.6$).

Matched performance			
K	20	40	80
P_d of the RCA-GLRT, SNR = 20 dB	0.010	0.650	0.997
P_d of the PRCA-GLRT, SNR = 20 dB	0.064	0.814	1.0
P_d of the RCA-ABORT, SNR = 20 dB	0.005	0.405	0.964
P_d of the PRCA-ABORT, SNR = 20 dB	0.041	0.566	0.975

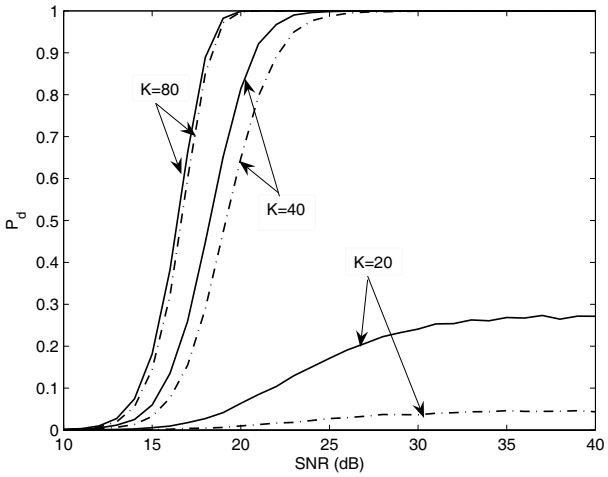

Figure 7. The matched performances of the PRCA-GLRT (solid line) and the RCA-GLRT (dashed-dotted line), for $N = 10$, $J = 4$, $\gamma = 0.6$, and several values of K.

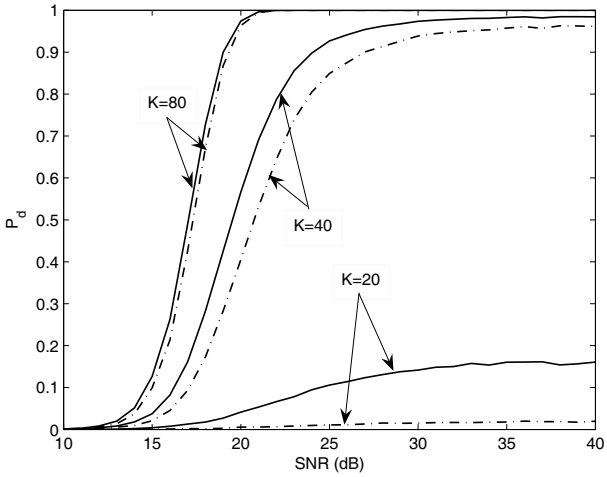

Figure 8. The matched performances of the PRCA-ABORT (solid line) and the RCA-ABORT (dashed-dotted line), for $N = 10$, $J = 4$, $\gamma = 0.6$, and several values of K.

4. CONCLUSIONS

In this paper, we have proposed tunable detectors for multiple point-like targets without a preassigned set of secondary data. First of all we have assumed that the useful signal belongs to a conic region and thus we have devised two adaptive GLRT-based detectors relying on the two-step GLRT-based design procedure. Computer simulations show that the new detectors can providing a wider range of performances with respect to their counterparts and with a limited loss in terms of P_d for matched signals. Two modified detector, coupled with the MLE of persymmetric covariance matrix, have also been considered. They can significantly outperform already proposed tunable receivers in the presence of a small number of range cells.

Further work may involve the analysis of the proposed detectors in a clutter-dominated non-Gaussian scenario.

ACKNOWLEDGMENT

This work was supported by the National Natural Science Foundation of China under Grant No. 61172166.

REFERENCES

1. Kelly, E. J., "An adaptive detection algorithm," *IEEE Transactions on Aerospace and Electronic Systems*, Vol. 22, No. 1, 115–127, 1986.
2. Robey, F. C., D. L. Fuhrman, E. J. Kelly, and R. Nitzberg, "A CFAR adaptive matched filter detector," *IEEE Transactions on Aerospace and Electronic Systems*, Vol. 29, No. 1, 208–216, 1992.
3. Conte, E., M. Lops, and G. Ricci, "Adaptive matched filter detection in spherically invariant noise," *IEEE Signal Processing Letters*, Vol. 3, No. 8, 248–250, 1996.
4. Pulsone, N. B. and C. M. Rader, "Adaptive beamformer orthogonal rejection test," *IEEE Transactions on Signal Processing*, Vol. 49, No. 3, 521–529, 2001.
5. Bandiera, F., A. De Maio, and G. Ricci, "Adaptive CFAR radar detection with conic rejection," *IEEE Transactions on Signal Processing*, Vol. 55, No. 6, 2533–2541, 2007.
6. Greco, M., F. Gini, and A. Farina, "Radar detection and classification of jamming signals belonging to a cone class," *IEEE Transactions on Signal Processing*, Vol. 56, No. 5, 1984–1993, 2008.
7. De Maio, A., "Robust adaptive radar detection in the presence of steering vector mismatches," *IEEE Transactions on Aerospace and Electronic Systems*, Vol. 41, No. 4, 1322–1337, 2005.
8. Bandiera, F., D. Orlando, and G. Ricci, *Advanced Radar Detection Schemes under Mismatched Signal Models*, Morgan & Claypool Publishers, USA, 2009.
9. Richmond, C. D., "Performance of the adaptive sidelobe blanker detection algorithm in homogeneous environments," *IEEE Transactions on Signal Processing*, Vol. 48, No. 5, 1235–1247, 2000.
10. Hao, C., B. Liu, S. Yan, and L. Cai, "Parametric adaptive radar detector with enhanced mismatched signals rejection capabilities," *EURASIP Journal on Advances in Signal Processing*, Vol. 2010, Article ID 375136, 11 pages, 2010.
11. Hao, C., B. Liu, and L. Cai, "Performance analysis of a two-stage Rao detector," *Signal Processing*, Vol. 91, No. 8, 2141–2146, 2011.
12. Park, J. I. and K. T. Kim, "A comparative study on ISAR imaging algorithms for radar target identification," *Progress In Electromagnetics Research*, Vol. 108, 155–175, 2010.
13. Huang, C. W. and K. C. Lee, "Application of ICA technique to

PCA based radar target recognition," *Progress In Electromagnetics Research*, Vol. 105, 157–170, 2010.

14. Han, S. K. and H. T. Kim, "Efficient radar target recognition using a combination of range profile and time frequency analysis," *Progress In Electromagnetics Research*, Vol. 108, 131–140, 2010.
15. Jia, Y., L. J. Kong, and X. B. Yang, "A novel approach to target localization through unknown walls for through-the-wall radar imaging," *Progress In Electromagnetics Research*, Vol. 119, 107–132, 2011.
16. Deng, H. and H. Ling, "Clutter reduction for synthetic aperture radar imagery based on adaptive wavelet packet transform," *Progress In Electromagnetics Research*, Vol. 29, 1–23, 2000.
17. Lee, K.-C., C.-W. Huang, and M.-C. Fang, "Radar target recognition by projected features of frequency-diversity RCS," *Progress In Electromagnetics Research*, Vol. 81, 121–133, 2008.
18. Qu, Y., G. Liao, S.-Q. Zhu, X.-Y. Liu, and H. Jiang, "Performance analysis of beamforming for MIMO radar," *Progress In Electromagnetics Research*, Vol. 84, 123–134, 2008.
19. Lee, K.-C., J.-S. Ou, and M.-C. Fang, "Application of SVD noise-reduction technique to PCAbased radar target recognition," *Progress In Electromagnetics Research*, Vol. 81, 447–459, 2008.
20. Habib, M. A., M. Barkat, B. Aissa, and T. A. Denidni, "CA-CFAR detection performance of radar targets embedded in 'non centered Chi-2' clutter," *Progress In Electromagnetics Research*, Vol. 88, 135–148, 2008
21. Yueh, S. H., J. A. Kong, J. K. Jao, R. T. Shin, H. A. Zebker, T. Le Toan, and H. Ottl, "K-distribution and polarimetric radar clutter," *Progress In Electromagnetics Research*, Vol. 3, 237–275, 1990.
22. Alyt, O. A. M., A. S. Omar, and A. Z. Elsherbeni, "Detection and localization of RF radar pulses in noise environments using waveletpacket transform and higher order statistics," *Progress In Electromagnetics Research*, Vol. 58, 301–317, 2006.
23. Bandiera, F., D. Orlando, and G. Ricci, "CFAR detection strategies for distributed targets under conic constraints," *IEEE Transactions on Signal Processing*, Vol. 57, No. 9, 3305–3316, 2009.
24. Besson, O., "Adaptive detection with bounded steering vectors mismatch angle," *IEEE Transactions on Signal Processing*, Vol. 55, No. 4, 1560–1564, 2007.
25. Bandiera, F., D. Orlando, and G. Ricci, "CFAR detection of

extended and multiple point-like targets without assignment of secondary data," *IEEE Signal Processing Letters*, Vol. 13, No. 4, 240–243, 2006.

26. Bandiera, F. and G. Ricci, "Adaptive detection and interference rejection of multiple point-like radar targets," *IEEE Transactions on Signal Processing*, Vol. 54, No. 12, 4510–4518, 2006.
27. Nitzberg, R., "Application of maximum likelihood estimation of persymmetric covariance matrices to adaptive processing," *IEEE Transactions on Aerospace and Electronic Systems*, Vol. 16, No. 1, 124–127, 1980.
28. Cai, L. and H. Wang, "A persymmetric multiband GLR algorithm," *IEEE Transactions on Aerospace and Electronic Systems*, Vol. 28, No. 3, 806–816, 1992.
29. Casillo, M., A. De Maio, S. Iommelli, and L. Landi, "A persymmetric GLRT for adaptive detection in partially-homogeneous environment," *IEEE Signal Processing Letters*, Vol. 14, No. 12, 1016–1019, 2007.
30. Pailloux, G., P. Forster, J. P. Ovarlez, and F. Pascal, "Persymmetric adaptive radar detectors," *IEEE Transactions on Aerospace and Electronic Systems*, Vol. 47, No. 4, 2376–2390, 2011.